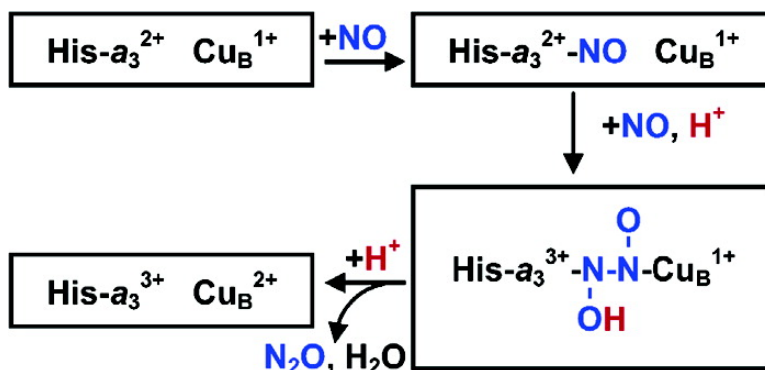


Detection of the His-Heme Fe–NO Species in the Reduction of NO to NO by *ba*-Oxidase from *Thermus thermophilus*

Eftychia Pinakoulaki, Takehiro Ohta, Tewfik Soulimane, Teizo Kitagawa, and Constantinos Varotsis

J. Am. Chem. Soc., **2005**, 127 (43), 15161-15167 • DOI: 10.1021/ja0539490 • Publication Date (Web): 04 October 2005

Downloaded from <http://pubs.acs.org> on March 25, 2009



More About This Article

Additional resources and features associated with this article are available within the HTML version:

- Supporting Information
- Links to the 7 articles that cite this article, as of the time of this article download
- Access to high resolution figures
- Links to articles and content related to this article
- Copyright permission to reproduce figures and/or text from this article

[View the Full Text HTML](#)

Detection of the His-Heme Fe²⁺–NO Species in the Reduction of NO to N₂O by *ba*₃-Oxidase from *Thermus thermophilus*

Eftychia Pinakoulaki,[†] Takehiro Ohta,[‡] Tewfik Soulimane,^{§,#} Teizo Kitagawa,[‡] and Constantinos Varotsis^{*†}

Contribution from the Department of Chemistry, University of Crete, 71409 Heraklion, Crete, Greece, Okazaki Institute for Integrative Bioscience, National Institutes of Natural Sciences, Okazaki, Aichi 444-8787 Japan, and Paul Scherrer Institute, Life Sciences, OSRA/008, CH-5232 Villigen PSI, Switzerland

Received June 15, 2005; E-mail: varotsis@edu.uoc.gr

Abstract: Reaction pathways in the enzymatic formation and cleavage of the N–N and N–O bonds, respectively, are difficult to verify without the structure of the intermediates, but we now have such information on the heme *a*₃²⁺–NO species formed in the reaction of *ba*₃-oxidase with NO from resonance Raman spectroscopy. We have identified the His-heme *a*₃²⁺–NO/Cu_B¹⁺ species by its characteristic Fe–NO and N–O stretching frequencies at 539 and 1620 cm⁻¹, respectively. The Fe–NO and N–O frequencies in *ba*₃-oxidase are 21 and 7 cm⁻¹ lower and higher, respectively, than those observed in Mb–NO. From these results and earlier Raman and FTIR measurements, we demonstrate that the protein environment of the proximal His384 that is part of the Q-proton pathway controls the strength of the Fe–His384 bond upon ligand (CO vs NO) binding. We also show by time-resolved FTIR spectroscopy that Cu_B¹⁺ has a much lower affinity for NO than for CO. We suggest that the reduction of NO to N₂O by *ba*₃-oxidase proceeds by the fast binding of the first NO molecule to heme *a*₃ with high-affinity, and the second NO molecule binds to Cu_B with low-affinity, producing the temporal co-presence of two NO molecules in the heme-copper center. The low-affinity of Cu_B for NO binding also explains the NO reductase activity of the *ba*₃-oxidase as opposed to other heme-copper oxidases. With the identification of the His-heme *a*₃²⁺–NO/Cu_B¹⁺ species, the structure of the binuclear heme *a*₃–Cu_B¹⁺ center in the initial step of the NO reduction mechanism is known.

Introduction

The thermophilic Gram-negative eubacterium *Thermus thermophilus* HB8 (ATCC27634) expresses *caa*₃- and *ba*₃-cytochrome oxidases.¹ In addition to their bioenergetic role of catalyzing the reduction of O₂ to H₂O and translocating protons across the inner bacterial membrane, both enzymes also catalyze the reduction of nitric oxide (NO) to nitrous oxide (N₂O) under reducing anaerobic conditions (*K*_m(NO) = 40 μM).^{1,2a} Thus, both enzymes, although their NO reductase activity is lower than the bona fide nitric oxide reductases (*K*_m(NO) = 1 nM), are both cytochrome oxidases and NO reductases.^{2a,b} Based on structural similarities between the *Pseudomonas stutzeri* NO reductases (Nor) and the *cbb*₃-cytochrome oxidase, it has been proposed that dioxygen (O₂) and nitric oxide (NO) can be used as alternative substrates by both enzyme superfamilies.^{2a} On the

same basis, it has been suggested that the essential difference between the two classes of enzymes lies in the organization of the active site. In the denitrification process, nitric oxide reductase (Nor) catalyzes the two-electron reduction of NO to N₂O through a heme *b*₃-non heme Fe dinuclear center, whereas in the respiratory enzyme the reduction of O₂ to H₂O takes place in a binuclear heme Fe–Cu_B center. The molecular mechanism of NO reduction in the bona fide reductases has not been fully investigated yet, and little is known about the mechanism in *cbb*₃-oxidase because it is difficult to obtain structural information on the state of NO in the various intermediates that are formed during its reduction.^{3–6} A full elucidation of the structure and the electron configuration of various intermediates are of profound importance for understanding the mechanism by which the enzymes form and cleave the N–N and N–O bonds, respectively.

The crystal structure of *ba*₃-cytochrome oxidase indicates that subunit I consists of a low-spin heme *b* and a high-spin heme *a*₃/Cu_B atom binuclear center where the dioxygen and nitric

[†] University of Crete.

[‡] National Institutes of Natural Sciences.

[§] Paul Scherrer Institute.

[#] Present address: Membrane Protein Structural Biology, College of Science, University of Limerick, Ireland.

- (1) Soulimane, T.; Buse, G.; Bourenkov, G. P.; Bartunik, H. D.; Huber, R.; Than, M. E. *EMBO J.* **2000**, *19*, 1766–1776.
- (2) (a) Giuffrè, A.; Stubauer, G.; Sarti, P.; Brunori, M.; Zumft, W. G.; Buse, G.; Soulimane, T. *Proc. Natl. Acad. Sci. U.S.A.* **1999**, *96*, 14718–14723.
(b) Hendriks, J.; Gohlke, U.; Saraste, M. *J. Bioenerg. Biomembr.* **1998**, *30*, 15–24.

- (3) Pinakoulaki, E.; Gemeinhardt, S.; Saraste, M.; Varotsis, C. *J. Biol. Chem.* **2002**, *277*, 23407–23413.

- (4) Pinakoulaki, E.; Varotsis, C. *Biochemistry* **2003**, *42*, 14856–14861.

- (5) Pinakoulaki, E.; Stavrakis, S.; Urbani, A.; Varotsis, C. *J. Am. Chem. Soc.* **2002**, *124*, 9378–9379.

- (6) Stavrakis, S.; Pinakoulaki, E.; Urbani, A.; Varotsis, C. *J. Phys. Chem. B* **2002**, *106*, 12860–12862.

oxide reactions take place, and subunit II contains a mixed-valence [$\text{Cu}_A^{1.5+}-\text{Cu}_B^{1.5+}$] homodinuclear copper complex.¹ The properties of the binuclear center of the CO-bound *ba*₃-oxidase have recently been characterized by optical absorption, FTIR, step-scan FTIR, and resonance Raman (RR) spectroscopy.^{7–14a} In our initial FTIR work, we demonstrated the existence of the equilibrium $\text{Cu}_B^{1+}-\text{CO}$ species and identified an input ligand channel at the Cu_B site.^{7,8} In a later study, we demonstrated the existence and the dynamics of a docking site near the propionate of the heme *a*₃ pyrrol ring A.^{9–12} Recently, we used RR spectroscopy to characterize the CO-bound complex of the fully reduced enzyme.^{13,14a} The RR spectra showed the formation of both a photolabile six-coordinate His384-heme Fe–CO and a photostable five-coordinate heme Fe–CO species, which is formed by the cleavage of the proximal heme Fe–His384 bond.¹³ The data indicated that the environment of the ruptured His384 that is a part of the Q-proton pathway and leads to the highly conserved among all heme-copper oxidases, H₂O pool, is disrupted upon CO binding to heme *a*₃. Furthermore, the detection of the $\nu(\text{CO})$ at 2053 cm^{-1} of the Cu_B-CO complex demonstrated the presence of a metal-to-ligand charge transfer (MLCT) transition.^{14a}

In this report, we have utilized optical absorption, time-resolved FTIR, and RR spectroscopy to characterize the reaction of fully reduced *ba*₃-oxidase with NO under steady-state conditions. We report the Fe–NO and N–O stretching modes of the ferrous nitrosyl six-coordinate, low-spin complex, and discuss the role of the proximal and distal residues in modulating the vibrational frequencies of the bound NO. We show that the $\nu(\text{Fe}-\text{NO})$ and $\nu(\text{NO})$ observed at 539 and 1620 cm^{-1} , respectively, are not affected by H₂O/D₂O exchanges in the pH 6–9 range, indicating that the immediate environment of the bound NO does not contribute to the weakening, as compared to ferrous nitrosyl Mb–NO, of the heme *a*₃ Fe–NO bond. The data from the low-spin NO-bound complex are in contrast to results obtained for the CO-bound complex that revealed the formation of both six- and five-coordinate heme *a*₃ Fe–CO species, and thereby define structural differences between the ferrous nitrosyl and carbon monoxide complexes. Our time-resolved step-scan FTIR data show that Cu_B , in contrast to its relatively high affinity for CO binding, has a low affinity for NO binding. To account for the detection of the nitrosyl intermediate, we propose a model describing the early molecular events in the NO reduction mechanism. In this model, NO activation in *ba*₃-oxidase occurs with a mixed valence form of the enzyme in which the low-potential site of the enzyme that is constituted by the low-spin heme *b* and Cu_A are oxidized, and the high potential site heme *a*₃ and Cu_B are reduced, providing the two electrons that are required for the reduction

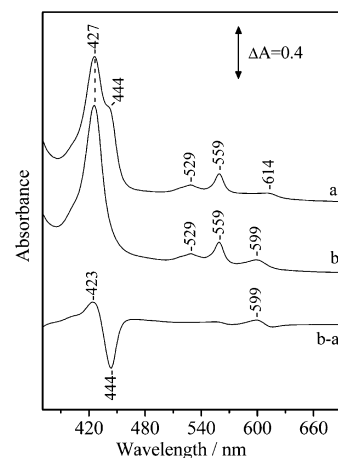


Figure 1. Optical absorption spectra of dithionite reduced *ba*₃-oxidase from *T. thermophilus* (spectrum a) and of the reduced NO-bound form (spectrum b). The difference spectrum (b – a) of the reduced NO-bound form minus the reduced indicates the binding of NO to heme *a*₃.

of NO to N₂O. Our model is supported by the detection of the high affinity His–Fe–NO intermediate, and from the absence of any modes that could be attributed to the formation of the Cu_B-NO species at 5 μs , the low-affinity of Cu_B for NO binding. Based on the crystal structure and our data, we also discuss the environment of the proximal heme Fe–His384/Asn366 pair in controlling the dynamics of the distal ligand binding.

Materials and Methods

Oxidized *ba*₃ enzyme was isolated from *T. Thermophilus* HB8 cells according to previously published procedures.¹ Dithionite (7 mM)-reduced samples were exposed to 1 atm NO in an anaerobic rotating quartz cell for the Raman measurements. The samples used for the RR measurements had an enzyme concentration of 50 μM and were placed in a desired buffer (pH 5.5–6.5, MES; pH 7.5, HEPES; pH 8.5–9.5 CHES). Under these conditions, turnover of the enzyme occurred and the stable heme $\text{Fe}^{2+}-\text{NO}$ Cu_B^{1+} species was formed for approximately 30 min. At later times, the fully oxidized enzyme was reformed. The resonance Raman spectra were acquired as described elsewhere.^{4,5,13,14a} The incident laser power of the 406.7 nm excitation frequency was 5 mW, and the total accumulation time was 30 min for each spectrum. The time-resolved step scan FTIR spectra were acquired as described elsewhere.^{4,7–12} ¹⁵NO was purchased from Isotec.

Results

The optical absorption spectrum of dithionite reduced *ba*₃ enzyme displays Soret maxima at 427 (heme b^{2+}) and 444 (heme a_3^{2+}) nm and visible maxima at 559 (heme b^{2+}) and 614 (heme a_3^{2+}) nm (Figure 1, spectrum a). Flushing NO over the reduced enzyme shifts the visible band of heme a_3^{2+} by 15 nm to 599 nm and the Soret at 427 nm has gained intensity (Figure 1, spectrum b), while the bands due to heme b^{2+} remained, as expected, unchanged. The difference spectrum (b – a) of the reduced NO-bound minus reduced form is characteristic of NO binding to heme *a*₃, as denoted by the peaks at 423 and 599 nm.^{14b,30} Addition of NO to the oxidized enzyme leads to the formation of the optical transitions at 437 and 587 nm (Varotsis et al. unpublished results).

- (7) Koutsoupakis, K.; Stavrakis, S.; Pinakoulaki, E.; Soulimane, T.; Varotsis, C. *J. Biol. Chem.* **2002**, *277*, 32860–32866.
- (8) Koutsoupakis, K.; Stavrakis, S.; Soulimane, T.; Varotsis, C. *J. Biol. Chem.* **2003**, *278*, 14893–14896.
- (9) Koutsoupakis, K.; Soulimane, T.; Varotsis, C. *J. Biol. Chem.* **2003**, *278*, 36806–36809.
- (10) Koutsoupakis, K.; Soulimane, T.; Varotsis, C. *J. Am. Chem. Soc.* **2003**, *125*, 14728–14732.
- (11) Koutsoupakis, C.; Soulimane, T.; Varotsis, C. *Biophys. J.* **2004**, *86*, 2438–2444.
- (12) Koutsoupakis, C.; Pinakoulaki, E.; Stavrakis, S.; Daskalakis, V.; Varotsis, C. *Biochim. Biophys. Acta* **2004**, *1655*, 347–352.
- (13) Ohta, T.; Pinakoulaki, E.; Soulimane, T.; Kitagawa, T.; Varotsis, C. *J. Phys. Chem. B* **2004**, *108*, 5489–5491.
- (14) (a) Pinakoulaki, E.; Ohta, T.; Soulimane, S.; Kitagawa, T.; Varotsis, C. *J. Biol. Chem.* **2004**, *279*, 22791–22794. (b) Rousseau, D. L.; Singh, S.; Ching, Y.-C.; Sassarolo, M. *J. Biol. Chem.* **1988**, *263*, 5681–5685.

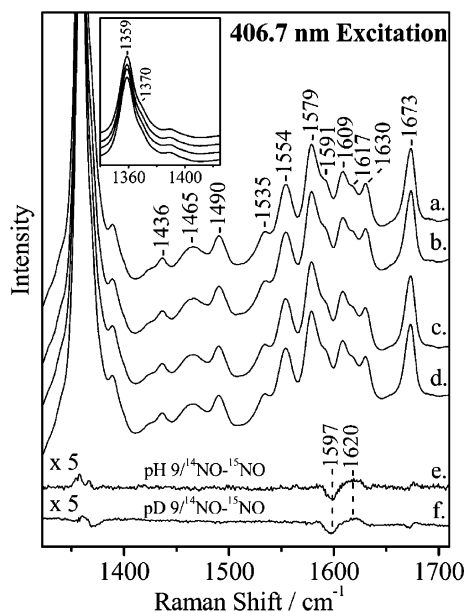


Figure 2. High-frequency resonance Raman spectra of dithionite reduced NO-bound ba_3 -oxidase at pH 9 (spectra a and b) and pD 9 (spectra c and d). Inset: the ν_4 region of the NO bound-complex at pH and pD 9. Spectra a and c are the ^{14}N -bound, and spectra b and d are the ^{15}N -bound. Spectrum e is the difference spectrum (a – b), and spectrum f is the difference spectrum (c – d). The excitation laser wavelength was 406.7 nm.

Figure 2 shows the high frequency data of the fully reduced ba_3 -oxidase at pH/pD 9 upon addition of NO and ^{15}NO . Spectra a (^{14}NO) and b (^{15}NO) are at pH 9, and spectra c (^{14}NO) and d (^{15}NO) are at pD 9. Spectra e and f are the difference spectra (a – b) and (c – d), respectively. The presence of modes at 1370 (ν_4) shown in the inset, and at 1490 (ν_3), 1591 (ν_2), and 1630 (ν_{10}) cm^{-1} upon addition of NO, indicate the formation of a six-coordinate low-spin heme a_3^{2+} species. The $\nu(\text{NO})$ frequency of ferrous nitrosyl-heme proteins and -heme model compound is observed in the 1590–1700 cm^{-1} frequency range.^{5,15–25} This spectral region in the RR spectra of ba_3 -oxidase is very congested, preventing us from observing the $\nu(\text{NO})$ stretching mode in the absolute spectra. The difference spectra, however, show the presence of a peak/trough pattern at 1620/1597 cm^{-1} in both the pH (spectrum e) and the pD 9 (spectrum f) experiments. The frequency of the 1620 cm^{-1} mode is in agreement with $\nu(\text{NO})$ frequencies observed in other six-coordinate low-spin ferrous nitrosyl heme proteins.^{15,16,21–25} The isotope shift (23 cm^{-1}) is also in agreement with that predicted

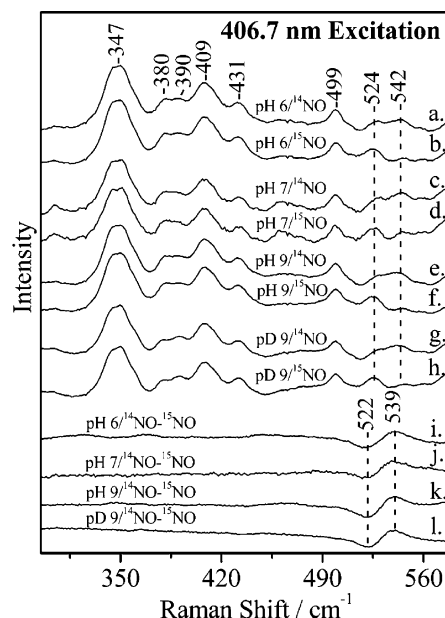


Figure 3. Low-frequency resonance Raman spectra of dithionite reduced NO-bound ba_3 -oxidase at the indicated pH and pD, and their corresponding difference spectra. The excitation laser wavelength was 406.7 nm.

(29 cm^{-1}) from the two body harmonic oscillator approximation. For example, the analogous $\nu(\text{NO})$ stretching mode in the RR spectra of Mb–NO is observed at 1613 cm^{-1} and the $^{14}\text{N}/^{15}\text{N}$ shift is 26 cm^{-1} ,¹⁵ the analogous isotope shift in the FTIR experiments is 30 cm^{-1} .^{16,25} This allows us to assign it to the $\nu(\text{NO})$ stretching frequency of the ferrous nitrosyl heme a_3^{2+} complex. The insensitivity of $\nu(\text{NO})$ to pH/pD exchange suggests the absence of H-bonding interaction of the bound NO.

The low-frequency region of the RR spectra of dithionite reduced ba_3 -oxidase upon addition of NO in the 6–9 pH range and at pD 9, obtained with 406.7 nm excitation, is shown in Figure 3. RR spectra of ferric and ferrous nitrosyl-heme protein and -heme model complexes exhibit the Fe–N–O vibrational modes in the 400–600 cm^{-1} spectral region.^{5,15,17–24} Spectra a, c, and e are the RR spectra of fully reduced ba_3 upon addition of NO at pH 6, 7, and 9, respectively. Spectra b, d, and f are the analogous RR spectra upon addition of ^{15}NO . Spectra g and h are the fully reduced RR spectra at pD 9 upon addition of NO and ^{15}NO , respectively. The absolute RR spectra in the 6–9 pH range and at pD 9 indicate the presence of a mode at 542 cm^{-1} that displays nitrogen isotopic sensitivity by shifting to 524 cm^{-1} in the spectra obtained upon addition of ^{15}NO . All of the difference spectra (spectra i–l), however, show the peak/trough at 539/522 cm^{-1} and confirm the presence of the isotope sensitive modes. This allows us to assign it as the Fe–NO stretching vibration, as the 17 cm^{-1} shift is in agreement with that expected from the two-body harmonic oscillator approximation for Fe^{2+} –NO, but more important it is in excellent agreement with $\nu(\text{Fe}^{2+}$ –NO) frequencies observed in other six-coordinate protein heme Fe^{2+} –NO complexes.^{15,21–24} For an Fe–NO diatomic model, a 6 cm^{-1} frequency shift is predicted for the $^{14}\text{N}^{16}\text{O}$ to $^{15}\text{N}^{16}\text{O}$ comparison for a linear structure, whereas for a bent structure, a 16 cm^{-1} shift is predicted. In ferrous Mb–NO a large shift was detected, consistent with a bent structure. We suggest, based on the isotope shift, that this is also the case of the heme Fe^{2+} –NO we have detected (see below). Although the bent heme Fe–NO configuration is a

- (15) Tomita, T.; Hirota, S.; Ogura, T.; Olson, J. S.; Kitagawa, T. *J. Phys. Chem. B* **1999**, *103*, 7044–7054.
- (16) Miller, L. M.; Padraza, A. J.; Chance, M. R. *Biochemistry* **1997**, *36*, 12199–12207.
- (17) Vogel, K. M.; Kozlowski, P. M.; Zgierski, M. Z.; Spiro, T. G. *J. Am. Chem. Soc.* **1999**, *121*, 9915–9921.
- (18) Lukat-Rodgers, G. S.; Rodgers, K. R. *Biochemistry* **1997**, *36*, 4178–4187.
- (19) Deinum, G.; Stone, J. R.; Babcock, G. T.; Marletta, M. A. *Biochemistry* **1996**, *35*, 1540–1547.
- (20) Igaroshi, J.; Sato, A.; Kitagawa, T.; Yoshimura, T.; Yamauchi, S.; Sagami, I.; Shimizu, T. *J. Biol. Chem.* **2004**, *279*, 15752–15762.
- (21) Andrew, C. R.; George, S. J.; Lawson, D. M.; Eady, R. R. *Biochemistry* **2002**, *41*, 2353–2360.
- (22) Karrow, D. S.; Pan, D.; Tran R.; Pellicena, P.; Presley, A.; Mathies, R. A.; Marletta, M. A. *Biochemistry* **2004**, *43*, 10203–10211.
- (23) Das, T. K.; Wilson, E. M.; Cutruzzola, F.; Brunori, M.; Rousseau, D. L. *Biochemistry* **2001**, *40*, 10774–10781.
- (24) Tomita, T.; Gonzalez, G.; Chang, A. L.; Ikeda-Saito, M.; Gilles-Gonzalez, M.-A. *Biochemistry* **2002**, *41*, 4819–4826.
- (25) Park, E. S.; Thomas, M. R.; Boxer, S. G. *J. Am. Chem. Soc.* **2000**, *122*, 12297–12303.

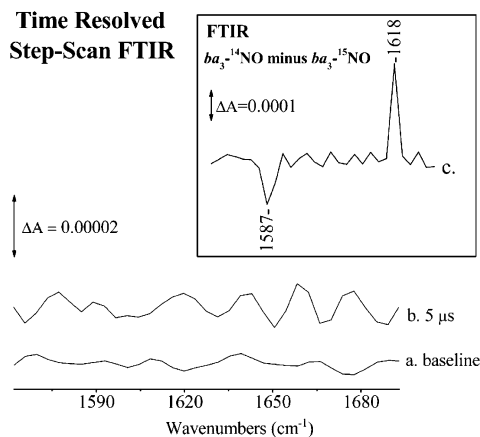


Figure 4. Inset: FTIR difference spectra of the ^{14}NO - minus ^{15}NO -bound ba_3 -oxidase at pH 7.5. Time-resolved step-scan (TRS²) FTIR (spectrum b) of fully reduced NO-bound ba_3 -oxidase at 5 μs after NO photolysis. The spectrum at 5 μs before the laser fires is included as a baseline (spectrum a). A 532 nm pump beam (5–10 mJ/pulse) at a repetition rate of 3 Hz was used for photolysis. The spectral resolution was 8 cm^{-1} .

character of the ferrous–NO complex, based on the crystal structure of ba_3 -oxidase, the bound ligand to heme a_3 is surrounded by two polar residues (His and Tyr237), which are ligands of Cu_B and can exert polar effects on the bound NO, and thus increase the Fe–NO bond order. The similarity of the $\nu(\text{Fe}^{2+}\text{–NO})$ in the 6–9 pH range and at pD 9 implies, however, just as in the case of Fe–CO complex,⁷ that there is no hydrogen-bonding interaction of the heme $\text{Fe}^{2+}\text{–NO}$ complex.

In the FTIR difference spectrum between the $^{14}\text{N}^{16}\text{O}$ - and $^{15}\text{N}^{16}\text{O}$ -bound states, shown in Figure 4 (inset), the positive peak at 1618 cm^{-1} is in agreement with that observed in the RR experiments, and thus it allows us to assign it to the $\nu(\text{NO})$ frequency. The negative peak at 1587 (^{15}NO), as well the 31 cm^{-1} isotope shift, are also in agreement with that predicted from the two-body harmonic oscillator approximation. Similar isotope shifts (30 cm^{-1}) have been observed in the low-temperature FTIR spectra of Mb–NO.¹⁶ There is a noticeable 8 cm^{-1} difference in the isotope shift between the FTIR (31 cm^{-1}) and RR data (23 cm^{-1}). We suggest that the Fermi resonance that occurs between the ν_2 vibration at 1590 cm^{-1} and the $\nu(^{15}\text{NO})$ in the RR spectra (Figure 2) upshifts the frequency of ^{15}NO from its intrinsic frequency, and thus a smaller isotope shift than predicted is observed. Similar coupling has been also observed in the RR spectra of Mb–NO in which the vibrational mixing of ν_2 with the ν_{NO} resulted in frequency shifts of both modes. However, in the absence of the ν_2 mode in our FTIR data, the 8 cm^{-1} difference in the isotope shift between the FTIR and RR data needs further investigation. No other modes are present in the spectra that could be attributed to a $\text{Cu}_B\text{–NO}$ complex. Therefore, we conclude that a single NO molecule is bound at the binuclear center. Figure 4 displays the TRS² FTIR difference spectrum of NO-bound state at 5 μs after NO photolysis. The absence of a negative peak at 1618 cm^{-1} demonstrates that full rebinding of NO to heme a_3 has occurred at 5 μs , and if the NO is coordinated to Cu_B upon photolysis from heme a_3 , then the lifetime of the $\text{Cu}_B^{1+}\text{–NO}$ complex is below our time-resolution of 5 μs .

As shown in Figure 5, the frequencies of $\nu(\text{Fe–NO})$ and $\nu(\text{NO})$ found in the NO-bound ba_3 -oxidase do not fall on the same correlation curve for five-coordinate species but rather

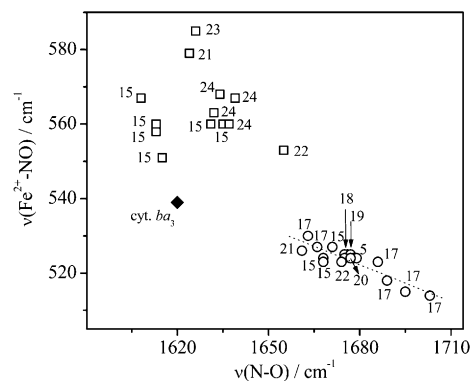


Figure 5. Correlation between frequencies of the Fe–NO versus the N–O stretching modes of five- and six-coordinate ferrous histidine-containing heme nitrosyl complexes. The circles are for five-coordinate complexes, and the squares are for six-coordinate complexes. The black diamond corresponds to the ferrous nitrosyl complex of ba_3 -oxidase. The numbering on the graph corresponds to the references. In the Supporting Information, a table with all heme-proteins and model complexes with their corresponding $\nu(\text{Fe–NO})$ and $\nu(\text{N–O})$ frequencies is provided.

lie close to the scattered values of the six-coordinate species. No correlation curve exists yet, for the six-coordinate Fe–N–O modes, and thus their frequencies do not reveal the identity of the proximal ligand. A well-established correlation curve exists for $\nu(\text{Fe–CO})$ and $\nu(\text{CO})$ that is distinctly different for proximal ligation by a thiolate versus that of a histidine because the proximal ligand affects the σ -orbital between the Fe and the C.²³ Although all of these proteins contain histidine as a proximal ligand, as in the case of ba_3 oxidase, their scattered values indicate that the identity of the proximal ligand cannot be determined from the $\nu(\text{Fe–NO})$ and $\nu(\text{NO})$ frequencies.

Discussion

The data reported here contain three major findings. First, the frequencies of $\nu_{\text{Fe–NO}}$ and $\nu_{\text{N–O}}$ modes of the primary intermediate in the reduction of NO to N_2O are identified in the RR spectra and are distinctly different from those observed in Mb–NO. Second, in a comparative study with our previous work, we demonstrate that the protein environment of the proximal H384 controls the strength of the Fe–His bond upon ligand (CO vs NO) binding to the Fe heme. Finally, Cu_B^{1+} has a much lower affinity for NO than for CO. Under this condition, the temporal co-presence of two NO molecules in the reduced binuclear center explains the observed NO reductase activity of the ba_3 -oxidase.

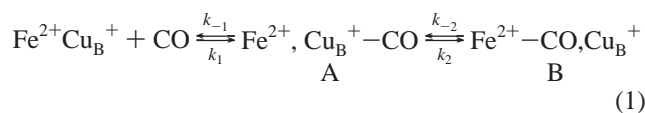
Properties of the His-Heme $\text{Fe}^{2+}\text{–NO}$ Species of ba_3 -Oxidase. Although it is well established that no correlation exists between $\nu(\text{Fe–NO})$ and $\nu(\text{N–O})$ in heme proteins, there is a general consensus that both proximal and distal effects control the properties of the NO bound ligand to heme proteins.^{15,16} In Mb–NO ($\nu_{\text{Fe–NO}} = 558 \text{ cm}^{-1}$, $\nu_{\text{NO}} = 1613 \text{ cm}^{-1}$), the heme Fe–N–O angle appears to be influenced by the strength of the proximal bond (Fe–His93) and the hydrogen-bonding interactions between the distal histidine (His64) and the bound NO.^{15,16} The strength of the Fe–His bond of deoxy Mb is medium ($\nu_{\text{Fe–His}} = 220 \text{ cm}^{-1}$) when compared to that of ba_3 ($\nu_{\text{Fe–His}} = 193/210 \text{ cm}^{-1}$) and of horseradish peroxidase ($\nu_{\text{Fe–His}} = 244 \text{ cm}^{-1}$).²⁶ An increase in the proximal bond length would predict

(26) Kitagawa, T. *Biological Applications of Raman Spectroscopy*; John Wiley & Sons: New York, 1998.

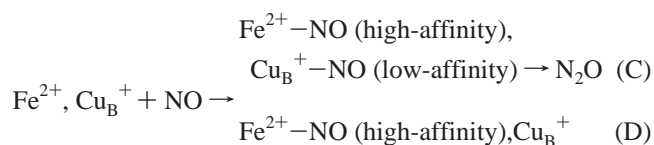
a decrease in the Fe–NO bond length and an increase in the Fe–N–O angle due to increasing π -bonding between the Fe and NO. Consequently, our data, in conjunction with the recent finding that the chemical environment of the binuclear center (pH 6–9, pD 5.5–10) does not alter the protonation state of the Cu_B ligands,^{8,11} indicate that the strength of Fe–NO and N–O bonds is controlled by the proximal His384 environment and its interaction with the protein. This way, the weaker Fe–His bond in ba_3 , as compared to Mb, increases the Fe–NO bond length producing a lower Fe–NO stretching frequency. On the other hand, the N–O stretching frequency is 7 cm^{-1} higher than that of Mb–NO. This observation is attributed to a decrease in electron density to the NO antibonding orbitals that results in strengthening the NO bond (higher ν_{NO}). Taken together, the observed Fe–NO and N–O stretching frequencies have a rationale in terms of $Fe(d_{\pi})$ –NO(π^*) bonding.

These results and those previously reported by others on the NO and CO binding to heme proteins^{15–25} lead to the suggestion that the lack of correlation between $\nu(Fe-NO)$ and $\nu(N-O)$, as opposed to $\nu(Fe-CO)$ and $\nu(C-O)$, is not only a consequence of the difference in their physical properties. Considering the scatter in the correlation in Figure 5 of the six-coordinate His–Fe–NO species, as opposed to the five-coordinate species, it can be concluded that the proximal environment affects the strength of the trans-ligand, and thus the $Fe(d_{\pi})$ –NO(π^*) bonding.

Binding of CO versus NO to Heme a_3 - Cu_B Center. The kinetics data on the photodissociation of CO and its rebinding to heme a_3 have shown that the CO-ligation/release mechanism in cytochrome ba_3 follows that found in other heme-copper oxidases, and proceeds according to the following scheme:



In contrast to the bovine aa_3 oxidase, Cu_B of cytochrome ba_3 has a relative high affinity for CO ($K_1 > 10^4$), whereas the transfer of CO to heme a_3^{2+} is characterized by a small $k_2 = 8 s^{-1}$, and by a $k_{-2} = 0.8 s^{-1}$ that is 30-fold greater than that of the bovine aa_3 .^{28,29} Therefore, 30% of heme a_3 remains unliganded upon CO binding to the enzyme.^{28,29} In contrast, the data presented here, and those reported previously on the reaction of reduced ba_3 -oxidase with NO, demonstrate that Cu_B has a low-affinity ($K_d \approx 40 \mu M$) for NO-binding and, thus, heme a_3 is fully ligated by NO forming a 6-c species under steady-state conditions.^{2a,30} Indeed, in the reduced NO-bound form of the enzyme under steady-state conditions, the Soret and visible optical absorption transitions are detected at 423 and 599 nm.³⁰ We propose that the NO-ligation and reduction mechanism in ba_3 -oxidase proceeds according to the following scheme:



In the formation of either complex C or D (steady state, excess NO), the heme nitrosyl species is the six-coordinate His-heme Fe–NO species we have detected. Of the heme-copper oxidases known, only the ba_3 -, caa_3 -, and the ccb_3 -oxidases display NO reductase activity.^{2,5,6} It is important to know that in mitochondrial aa_3 oxidase the copresence of two NO molecules has been demonstrated by FTIR measurements but the NO reductase activity is virtually 0%.²⁷ Consequently, the co-presence of two NO molecules in the binuclear center is not a prerequisite for NO activity. This indicates that the NO binding constant (K) of Cu_B controls the NO activity by heme-copper oxidases.

Dynamics of the H384/Asn366 Environment upon Ligand Binding. The distance of the heme a_3 Fe to the proximal histidine ligand (His384/ $\alpha 10$) is 3.3 Å (Fe–N_e), considerably larger than that found in *P. denitrificans* and bovine heart oxidases.¹ Furthermore, the distance from N_δ of His384 to the carbonyl of Gly359 is 3.43 Å (H-bonding distance), and the distance of N_e of H384 to Asn366 (N side chain) is 3.02 Å.¹ The $\nu(Fe-His)$ of ba_3 -oxidase at 193/210 cm^{-1} ¹³ is close to that observed in other histidine-coordinated heme proteins such as HbA (T-state, $\nu_{Fe-His} = 207$), sGC ($\nu_{Fe-His} = 204 cm^{-1}$), and FixL ($\nu_{Fe-His} = 209 cm^{-1}$) in which the proximal histidine is detached upon NO binding.^{5,18,19,26} Coordination of NO to heme a_3 , however, leaves the proximal His384 intact. Obviously, the proximal heme environment controls the dynamics of the Fe–His384 bond strength upon ligand binding to the heme a_3 Fe.

Two $\nu(Fe-His)$ conformers have been detected in the RR data of ba_3 -oxidase.¹³ The variation in the hydrogen-bonding state of the proximal heme Fe–His384 with Gly359 has been invoked to account for the occurrence of the split Fe–His stretching mode, which has components at 193 and 210 cm^{-1} . The conformer with the weaker (or absent) H-bond has the weaker Fe–His bond and the lower frequency vibration at 193 cm^{-1} . The more strongly H-bonded conformer contributes to the 210 cm^{-1} . To account for the observation of the photostable five-coordinate Heme Fe–CO species, and on the basis of the crystal structure, we suggested that upon CO binding there is a communication linkage between Asn366 and His384 that causes the rupture of the Fe–His384 bond.¹³ The CO-photostationary experiments have also revealed that the non-hydrogen bonded conformer is diminished and the intensity of the H-bonded conformer has increased. In the case of NO binding, we have not detected the formation of a five-coordinate species. This provides strong evidence that NO binding to the Fe heme a_3 shifts the His–Fe–NO conformational equilibria toward the H-bonded proximal H384 conformer, stabilizing the six-coordinate His–Fe–NO species we have detected. Communication linkage between the distal and proximal sides through hydrogen bond networks has been suggested to occur in HRP, aa_3 -600, and aa_3 from *P. denitrificans*.^{31–33} It is tempting to

(27) Zhao, X. J.; Sampath, V.; Caughey, W. S. *Biochem. Biophys. Res. Commun.* **1994**, *204*, 537–543.

(28) Goldbeck, R. A.; Einarsdóttir, O.; Dawes, T. D.; O'Connor, D. B.; Surer, K. K.; Fee, J. A.; Kligler, D. S. *Biochemistry* **1992**, *31*, 9376–9387.

(29) Giuffrè, A.; Forte, E.; Antonini, G.; D'Itri, E.; Brunori, M.; Soulimane, T.; Buse, G. *Biochemistry* **1999**, *38*, 1057–1065.

(30) Pilet, E.; Nitschke, W.; Rappaport, F.; Soulimane, T.; Lambry, J.-C.; Liebl, U.; Vos, M. H. *Biochemistry* **2004**, *43*, 14118–14127.

(31) Mukai, M.; Nagano, S.; Tanaka, M.; Ishimori, K.; Morishima, I.; Ogura, T.; Watanabe, Y.; Kitagawa, T. *J. Am. Chem. Soc.* **1997**, *119*, 1758–1766.

(32) Varotsis, C.; Vamvouka, M. *J. Phys. Chem.* **1998**, *102*, 7670–7673.

(33) Pinakoulaki, E.; Pflitzner, U.; Ludwig, B.; Varotsis, C. *J. Biol. Chem.* **2003**, *278*, 18761–18766.

conclude that this conformational change at the proximal-side can act as a control mechanism for the coordination and redox chemistry of heme a_3 . Because the environment of Cu_B in ba_3 -oxidase is not altered in the pH 5–10 range, the communication linkage is not the result of structural changes of the Cu_B atom and its associated ligands including the cross-link His-Tyr237, but rather conformational changes induced to the environment of Cu_B by the incoming ligand. Such conformational changes induced by O_2 in the O_2 channel to Cu_B have been demonstrated recently.⁸ These observations are also in agreement with our previous conclusions that the properties of the O_2 channel that is located at the Cu_B site are not limited to facilitate ligand diffusion to the active site, but are extended in controlling the dynamics and reactivity of the reactions of ba_3 with O_2 , CO , and NO .⁸

Structural Concepts of the Catalytic Sites in NO Reductases. The two-electron reduction of NO to N_2O involves the formation of the N–N bond and the cleavage of N–O bond. However, the reduction mechanism by Nor and the heme-copper reductases is largely hypothetical. It has been demonstrated that NO reductase activity is sustained by ferric heme (P450Nor), the di-nuclear center of Nor, and the binuclear active site of ba_3 -oxidase.^{2,33–35} Both the non-heme Fe in Nor and the Cu_B in ba_3 -oxidase have a low affinity for NO .^{3,4}

In the case of Nor, the midpoint redox potentials of each of the metal centers in the enzyme have been measured, and from the unexpectedly low midpoint redox potential of heme b_3 ($E_m = 60$ mV) it was suggested that full reduction of the di-nuclear center is thermodynamically unfavorable.³⁶ The redox potentials of the other redox centers were reported at 310 mV for Fe(II) heme c , 345 mV for Fe(II) heme b , and 320 mV for the non-heme Fe(II).³⁶ Based on the redox potentials, we proposed that it is possible that under physiological conditions, NO activation in Nor occurs with a mixed valence form of the enzyme in which the low-spin hemes b and c and the non-heme Fe are reduced, and heme b_3 is in the oxidized form.³ This way, a single molecule of NO binds at the heme b_3 , and addition of two electrons to heme b_3 Fe^{3+} – NO yields the two electron reduced species Fe^{2+} – $\text{N}=\text{O}^-$. A second NO molecule attacks the N atom of the ferrous– NO species to transiently yield hyponitrite (HONNO^-), and thus the N–N bond formation. Cleavage of the N–O bond produces the ferric enzyme, N_2O , and H_2O . Recently, under single turnover conditions, a five-coordinated heme– NO species was detected by EPR.³⁷

In ba_3 -oxidase, however, reduction of the binuclear heme a_3 – Cu_B^{1+} center is favorable,³⁸ and thus we propose that the NO reduction mechanism occurs in the reduced binuclear heme a_3 – Cu_B center. To account for the possible ligand-binding states upon addition of NO to ba_3 -oxidase, we propose the mechanism shown in Figure 6. In the mechanism, we propose that the two electrons required for the NO catalytic cycle are supplied by the reduced heme Fe^{2+} – Cu_B^{1+} binuclear center. Addition of

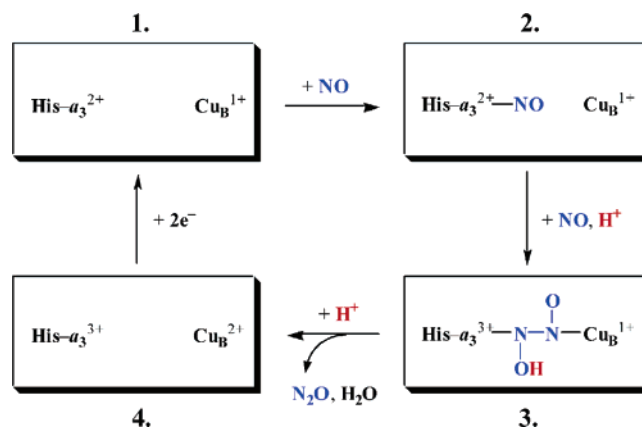


Figure 6. Proposed mechanism for the reduction of NO to N_2O by ba_3 -oxidase (see text).

NO to heme a_3^{2+} – Cu_B^{1+} produces the primary His-heme a_3 Fe– NO species we have detected (2). A second NO molecule binds to Cu_B with low-affinity attacking the N atom of the ferrous-heme Fe– NO species; protonation occurs to transiently yield hyponitrite (HONNO^-), and thus the N–N bond formation (3). This form of the enzyme is unstable to oxidation and with the addition of H^+ is leading to form 4 and the concomitant production of N_2O and H_2O . In our experiments on the fully reduced- NO ba_3 enzyme, we find no evidence for any oxidized components, suggesting that sufficient dithionite is present in our samples to prevent formation of any oxidized species. Therefore, the formation of hyponitrite 3 from heme a_3^{2+} – NO 2, which depends on excess NO , should be inhibited under our conditions, and the fully reduced His-heme Fe²⁺– NO 2 (complex D) becomes the dominant species under our reducing conditions. It should be noted that formation of N_2O can occur without the bridging reductants between the heme Fe and Cu_B .⁵ In this alternative mechanism, the second NO molecule attacks the N atom of the ferrous– NO species we have detected and protonation occurs to transiently yield the hyponitrite (HONNO^-), and thus the N–N bond formation.

Conclusions

The present work reports the detection of His-heme a_3^{2+} – $\text{NO}/\text{Cu}_B^{1+}$ species in the reduction of NO to N_2O by ba_3 -oxidase, which until now had not been detected in the bona fide NO reductases. Our data also demonstrate that the NO binding constant (K) of Cu_B controls the NO activity by heme-copper oxidases. From these results and earlier Raman and FTIR measurements, we demonstrate that the protein environment of the proximal histidine that is a part of the Q-proton pathway controls the strength of the Fe–His384 bond upon ligand (CO vs NO) binding. This proton channel leads through His384, Asn366, Asp372, and the propionate of the heme a_3 pyrrole ring A to an accumulation of H_2O molecules. Experiments that will determine the formation of the N–N bond and the cleavage of the N–O bond will be useful in elucidating the mechanism of these fascinating enzymes, and will be a useful starting point to have a clue of the proposed hypothesis of a common evolutionary origin of aerobic respiration and bacterial denitrification.^{2,39,40}

- (34) Obayashi, E.; Tsukamoto, K.; Adachi, S.-I.; Takahashi, S.; Nomura, M.; Iizuka, T.; Shoun, H.; Shiro, Y. *J. Am. Chem. Soc.* **1997**, *119*, 7807–7816.
- (35) Hendriks, J.; Warne, A.; Gohlke, U.; Haltia, T.; Ludovici, C.; Lubben, M.; Saraste, M. *Biochemistry* **1998**, *37*, 13102–13109.
- (36) Grönberg, K. L. C.; Roldan, M. D.; Prior, L.; Butland, G.; Cheesman, M. R.; Richardson, D. J.; Spiro, S.; Thomson, A. J.; Watmough, N. J. *Biochemistry* **1999**, *38*, 13780–13786.
- (37) Kumita, H.; Matsuura, K.; Hino, T.; Takahashi, S.; Hori, H.; Fukumori, Y.; Morishima, I.; Shiro, Y. *J. Biol. Chem.* **2004**, *279*, 55247–55254.
- (38) Hellwig, P.; Soulimane, T.; Buse, G.; Mantele W. *Biochemistry* **1999**, *38*, 9648–9658.

(39) Pinakoulaki, E.; Pfitzner, U.; Ludwig, B.; Varotsis, C. *J. Biol. Chem.* **2002**, *277*, 13563–13568.

(40) Pinakoulaki, E.; Soulimane, T.; Varotsis, C. *J. Biol. Chem.* **2002**, *277*, 32867–32874.

Acknowledgment. This work was supported by the Greek Secretariat of Research (C.V.), and by Grant-in-aids for Specifically Promoted Research from the Ministry of Education, Science, Sports and Culture, Japan (T.K., 14001004). C.V. thanks Irene Gialou for preliminary data. T.O. thanks JSPS for a research fellowship.

Supporting Information Available: Table for five- and six-coordinate ferrous nitrosyl heme-protein and model complexes with their corresponding $\nu(\text{Fe}-\text{NO})$ and $\nu(\text{N}-\text{O})$ frequencies. This material is available free of charge via the Internet at <http://pubs.acs.org>.

JA0539490